



UDC 539.42

<https://doi.org/10.23947/2687-1653-2021-21-2-133-142>

Finite element modeling of the joint action of flow slide and protective structure



P. P. Gaidzhurov, N. A. Saveleva, V. A. Dyaiachenkov

Don State Technical University (Rostov-on-Don, Russian Federation)

Introduction. In the context of the problem of plane deformation, a finite-element model of a natural landslide slope is developed. It allows for the joint work of a flow slide and a protective engineering structure. The Drucker-Prager model is used to take into account the physical nonlinearity of the slope layer material. To activate the kinematic instability, a viscoelastic interlayer is introduced into the design scheme, along which the landslide layer slides.

Materials and Methods. Numerical experiments were performed using the ANSYS Mechanical software package, which implements the finite element method in the form of the displacement method. Slope discretization is performed on the basis of PLANE42 flat four-node finite elements. To simulate the displacement of the landslide layer relative to the fixed base, the combined viscoelastic elements COMBIN14 were used.

Results. A physically nonlinear model of a natural landslide slope consisting of a base, a landslide layer, and a viscoelastic interlayer, is formalized. An engineering technique for analyzing the stress-strain state of the “slope-protective structure” system has been developed, taking into account the kinematic instability of the landslide layer. A series of computational experiments was carried out.

Discussion and Conclusion. Based on the calculations performed, it is shown that the proposed method enables to specify the force action of the landslide layer on the protective structure and, thereby, to increase the reliability of the risk assessment when activating the landslide process.

Keywords: finite element method, Drucker-Prager model, landslide process simulation, landslide protection engineering structures.

For citation: P. P. Gaidzhurov, N. A. Saveleva, V. A. Dyaiachenkov. Finite element modeling of the joint action of flow slide and protective structure. *Advanced Engineering Research*, 2021, vol. 21, no. 2, pp. 133–142. <https://doi.org/10.23947/2687-1653-2021-21-2-133-142>

© Gaidzhurov P. P., Saveleva N. A., Dyaiachenkov V. A., 2021



Introduction. The design of anti-landslide engineering structures is one of the most important areas in the construction science. At the same time, numerical modeling of the stability of natural landslide slopes is associated with uncertainty factors, such as instability of the physical and mechanical characteristics of the material and the variability of the fracture trajectories.

Nowadays, various variants of the limit equilibrium method and the method of reducing the shear strength of the material in combination with the finite element method are used to assess the slope stability [1–3]. The calculation result of the using the limit equilibrium method is the geometry of the “classical” circular sliding line. The method of reducing the strength provides more complete information about the sliding surface for the considered landslide area.

Particularly, we can distinguish the direction of the study of slope processes based on the model of the centroidal motion of particles that elastically interact with each other and the inclined surface [4]. Another approach based on block kinematics is the so-called discontinuous deformation analysis (DDA) method [5]. The DDA method has limitations regarding the interaction between adjacent blocks. The essence of these restrictions is the impossibility

of mutual penetration of the blocks and the absence of tensile stresses between the blocks. Figure 1 (taken from [5]) shows the block coupling scheme used in the ADD method for modeling rockfalls. In this Figure, k_x , k_y and c_x , c_y — are the stiffness and viscosity parameters, respectively, in the direction of the axes X and Y .

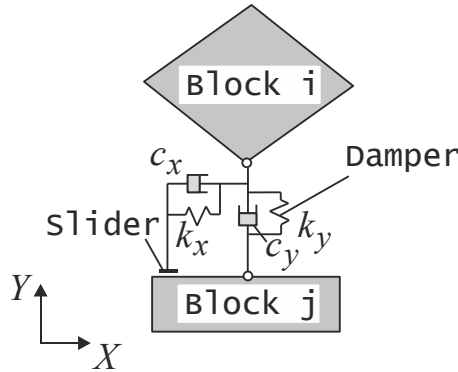


Fig. 1. Block diagram for modeling rockfalls

The disadvantage of the DDA method is the impossibility of introducing engineering structures into the design scheme that prevent the progressive destruction of the mountain range.

If, after assessing the natural slope stability, a decision is made on the feasibility of constructing landslide structures, then the data of engineering and geological surveys, as well as various scenarios of external force impacts on the landslide slope sections, are used as initial information for the design. Numerical simulation of the stress-strain state of a reinforced landslide slope is usually performed in a two-dimensional formulation within the framework of the nonlinear theory of elasticity using the finite element method. The ground pressure is assumed to be linearly distributed in depth. For engineering geotechnical calculations, specialized finite element software systems are used: Plaxis, MIDAS GTS, GEO5, which include the most common soil models. Modeling of complex geotechnical systems is carried out on the basis of the “heavy” software package ANSYS Mechanical [6].

It should be noted that in the papers devoted to the analysis of the stress-strain state of anti-landslide structures, there is no information on the use of models that take into account the direct sliding (creeping) of the landslide layer. In normal practice, design schemes are used, in which the joint (continuous) deformation of the entire soil mass is provided, up to the loss of the bearing capacity of the soil. This does not allow us to fully assess the force impact of the landslide layer on the structural elements.

Materials and Methods. The design scheme of the landslide slope is shown in Fig. 2 (dimensions are given in meters). Consider that the slope consists of two layers: S_1 — base of the slope (dense clay); S_2 — landslide layer (waterlogged loam). We assume that the position of the sliding line is known. The external impact is presented by the self-weight of the landslide layer S_2 and the evenly distributed pressure q .

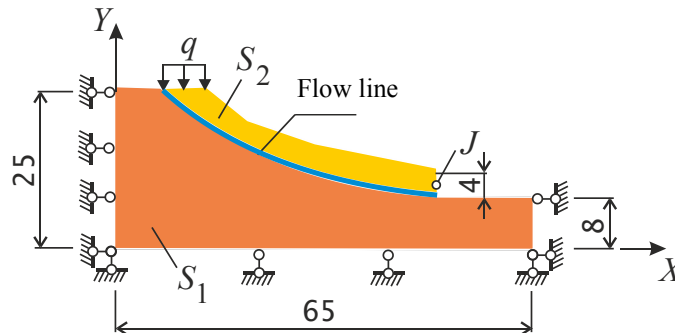


Fig. 2. Design scheme of landslide slope (dimensions are in meters)

The mechanical characteristics of the layer materials are given in Table 1.

Table 1

Mechanical characteristics of slope layers

Material	Deformation module E , MPa	Poisson's ratio ν	Angle of internal friction ϕ , deg.	Adhesion c , kPa	Density ρ , kg/m ³
layer S_1	21	0.30	15	45	1702
layer S_2	12	0.35	22	22	1800

Numerical simulation is performed using the ANSYS Mechanical software package. The finite element model of the slope is shown in Fig. 3. Two-dimensional 4-node finite elements PLANE42 are used for soil modeling. Moreover, the meshes of the layers S_1 and S_2 are topologically unrelated, i.e., along the flow line, each node has a double numbering. This will ensure to model the possible displacement of the layer S_2 relative to the layer S_1 .

To describe the behavior of the slope layers, we use the Drucker-Prager model of an elastic-perfectly-plastic material [7], which is included in the ANSYS Mechanical complex. The equation of the yield surface for this model has the form

$$F = \tau_i + 3\beta\sigma_m - \sigma_y = 0,$$

where τ_i — intensity of tangential stresses; σ_m — mean stress; β , σ_y — model parameters related to material constants C and ϕ ratios:

$$\beta = \frac{2 \sin \phi}{\sqrt{3}(3 - \sin \phi)}; \quad \sigma_y = \frac{6C \cos \phi}{\sqrt{3}(3 - \sin \phi)}.$$

Physical dependence linking stress and deformations for an elastic-perfectly-plastic material is described by the expression [8]

$$\tau_i = \frac{G \gamma_i}{1 + \gamma_i G / \tau_{np}},$$

where γ_i — the intensity of shear deformations; G — the shear modulus; the tangential stress corresponding to the material tensile strength (Fig. 4)

$$\tau_{np} = C + \sigma_m \operatorname{tg} \phi.$$

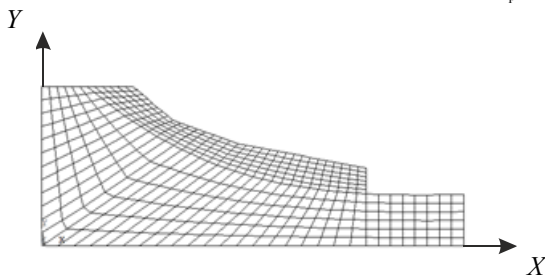


Fig. 3. Finite element model of the slope

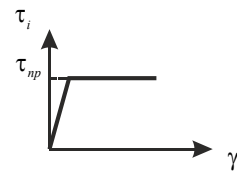


Fig. 4. Graph $\tau_i \sim \gamma_i$

The effect of possible sliding of the layer S_2 relative to the layer S_1 is modeled using combined elements (CE) of spring type COMBIN14 (Fig. 5).

The equilibrium equation for a combined spring element (CE) has the form

$$[h]\{u\} = \{p\},$$

where $[h]$ — stiffness matrix; $\{u\}$, $\{p\}$ — vectors of the columns of nodal displacements and forces. Depending on the orientation of the spring element, we have:

— local CE axis ξ coincides with the axis x

$$[h] = k_x \begin{bmatrix} 1 & 0 & -1 & 0 \\ 0 & 0 & 0 & 0 \\ -1 & 0 & 1 & 0 \\ 0 & 0 & 0 & 0 \end{bmatrix}; \quad \begin{aligned} \{u\} &= \{u_{ix} \ 0 \ u_{jx} \ 0\}^T; \\ \{p\} &= \{p_{ix} \ 0 \ p_{jx} \ 0\}^T. \end{aligned}$$

— local CE axis ξ coincides with the axis y

$$[h] = k_y \begin{bmatrix} 0 & 0 & 0 & 0 \\ 0 & 1 & 0 & -1 \\ 0 & 0 & 0 & 0 \\ 0 & -1 & 0 & 1 \end{bmatrix}; \quad \begin{aligned} \{u\} &= \{0 \ u_{iy} \ 0 \ u_{jy}\}^T; \\ \{p\} &= \{0 \ p_{iy} \ 0 \ p_{jy}\}^T. \end{aligned}$$

Here, k_y, k_x — stiffness coefficients corresponding to the orientations of the spring along the axes x and y ;

T — symbol of the transpose operation.

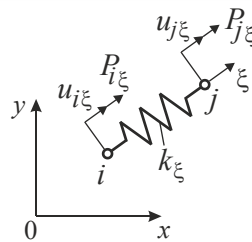


Fig. 5. Combined finite element COMBIN14

We take the following values of the elasticity coefficients:

$$k_y = 21 \text{ H/M}, \quad k_x = 100 \text{ H/M}.$$

Viscosity parameters: $c_x = c_y = 0.5 \text{ N}\cdot\text{s/m}$.

When assigning coefficients k_y and k_x , the aim was to bring the model of the slope under consideration closer to reality. In particular, along the flow line, we consider the shear strain resistance and elastic rebound of layer S_2 . A similar approach to modeling the “slipping” effect was used in [9]. Note that in the accepted layer discretization, the nodes i and j , belonging to the spring elements coincide. The design load includes the self-weight of the layer S_2 and the evenly distributed force q applied to the upper end of layer S_2 (Fig. 2).

To organize the computational process, we use the nonlinear “solver” of the ANSYS Mechanical complex, which implements the Newton-Raphson method.

To verify the finite element model, we estimate the slope stability under consideration through excluding the COMBIN14 elements from the design scheme and thus obtaining an unreduced model. By calculation, it is established that for an unweakened slope, the pressure limit value q , for the given mechanical characteristics of layers S_1 and S_2 , is 400 kPa. The operation process of the nonlinear solver is shown in the form of a graph in Fig. 6. Here, along the abscissa axis, the total number of iterations at each step of “Time” loading is plotted, along the ordinate axis, the corresponding norms of the residual forces “F” and displacements “U” are plotted. The “Time” parameter ranges from 0 to 1. The iterative process continues until the values “F”–“L2” are less than the values “F”–“CRIT”. The intersection of the peak of the sawtooth curve “F”–“L2” and the curve “F”–“CRIT” indicates that, in this example, the iterative process “converged” with the specified accuracy.

Figure 7 shows a picture of the distribution of horizontal displacements u_x in the body of an unweakened slope at $q = 400 \text{ kPa}$. As follows from the Figure, the loss of stability of the slope is local in nature. In this case, the circular-cylindrical type of the flow line is clearly traced. The corresponding distribution of the intensity field of plastic shear deformation γ_i is shown in Fig. 8.

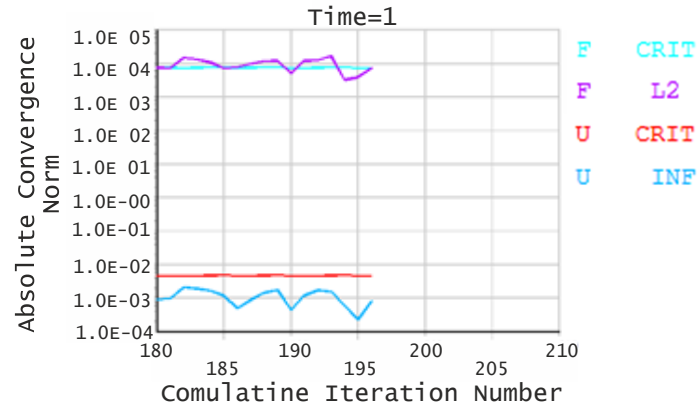


Fig. 6. Convergence graph of the Newton-Raphson procedure

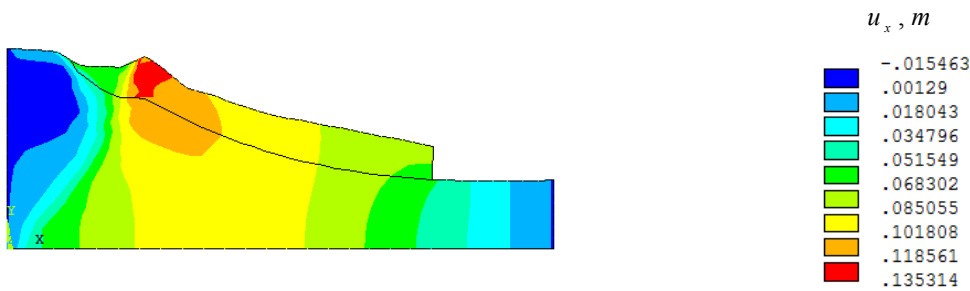


Fig. 7. Visualization of displacements u_x at $q=400$ kPa

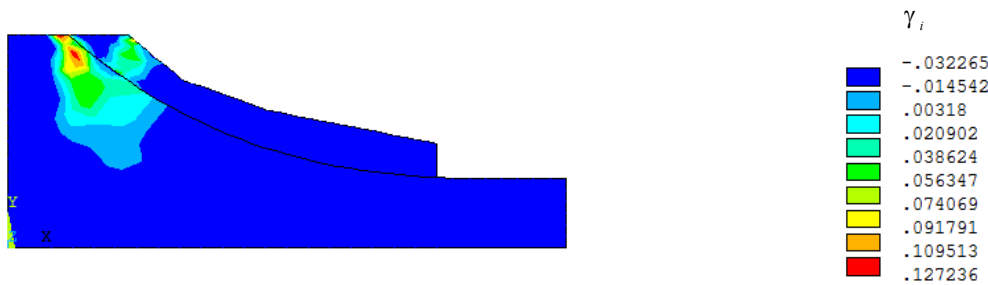


Fig. 8. Visualization of distribution γ_i at $q=400$ kPa

Research Results. To simulate the effect of kinematic instability of the landslide layer S_2 , we analyze the stress-strain state of the slope taking into account the weakening at different pressure values q . We emphasize that in this case, the elements of COMBIN14 are included. Fig. 9 shows the graph $u_x \sim q$, where u_x — the horizontal displacement of point J of the “tongue” of the landslide layer S_2 (Fig. 2).

Comparing the results of calculations for weakened and unweakened slopes, we come to the conclusion that the inclusion of a sliding layer in the design model significantly (by more than one order of magnitude) reduces the limit value q .

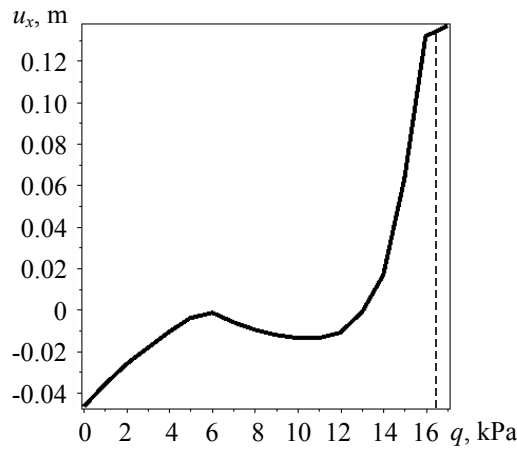


Fig. 9. Graph of the dependence of horizontal movement of point J of the “tongue” of landslide layer S_2 on pressure value q

The graph $u_x \sim q$ shows that, for the considered slope model, the landslide process has a pronounced nonlinear character. Moreover, in the pressure range from 6 kPa to 11 kPa, there is a displacement of the “tongue” of layer S_2 in the opposite direction to the expected landslide process. Fig. 10 shows a contrasting pattern of the distribution of the displacement field in the x - axis direction corresponding to the loading of layer S_2 with pressure $q=16.5$ kPa.

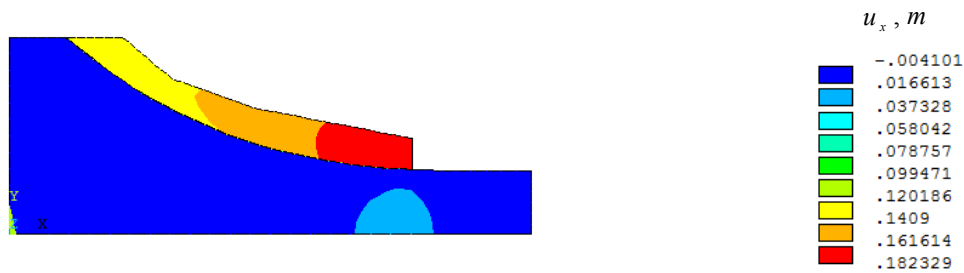


Fig. 10. Visualization of displacements u_x at $q=16.5$ kPa

A fragment of a finite element model of a landslide “tongue” in a deformed state at $q=16.5$ kPa is shown in Fig. 11.

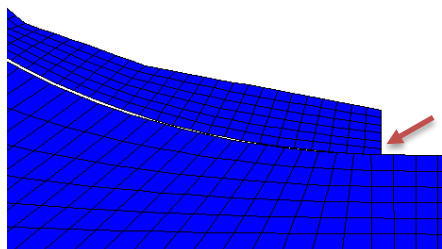


Fig. 11. Visualization of a finite element model of a slope fragment in a deformed state at $q=16.5$ kPa

As can be seen from Fig. 11, the proposed method allows you to simulate the effect of sliding of layer S_2 relative to layer S_1 . This effect is shown in the relative displacement of the grid nodes (shown by the arrow). Maximum relative displacement $u_{x\max}$ reaches 18.2 cm, which, from a physical point of view, is quite consistent with the landslide process onset.

Fig. 12 shows the considered variants of schemes of anti-landslide structures made of concrete. The following mechanical constants for concrete are accepted: $E_c = 3 \cdot 10^4$ MPa; $\nu_c = 0.2$; $\rho_c = 2446$ kg/m³. The design value of the height of the protective structures $h=2.6$ m. The depth of the pile foundation is 8 m (schemes b and c). Pressure value

$q = 16.5 \text{ kPa}$.

The pile foot (scheme *b*) and the sheet piling (scheme *c*) are presented by 2-node beam elements BEAM3. The diameter of the piles is assumed to be 0.35 m.

The visualization of the considered schemes of anti-landslide structures in the deformed state is shown in Fig. 13. From the above data, it follows that when modeling the landslide process, the “tongue” of layer S_2 is pressed into the foundation S_1 . This explains the “collapse” of anti-landslide structures towards the movement of layer S_2 .

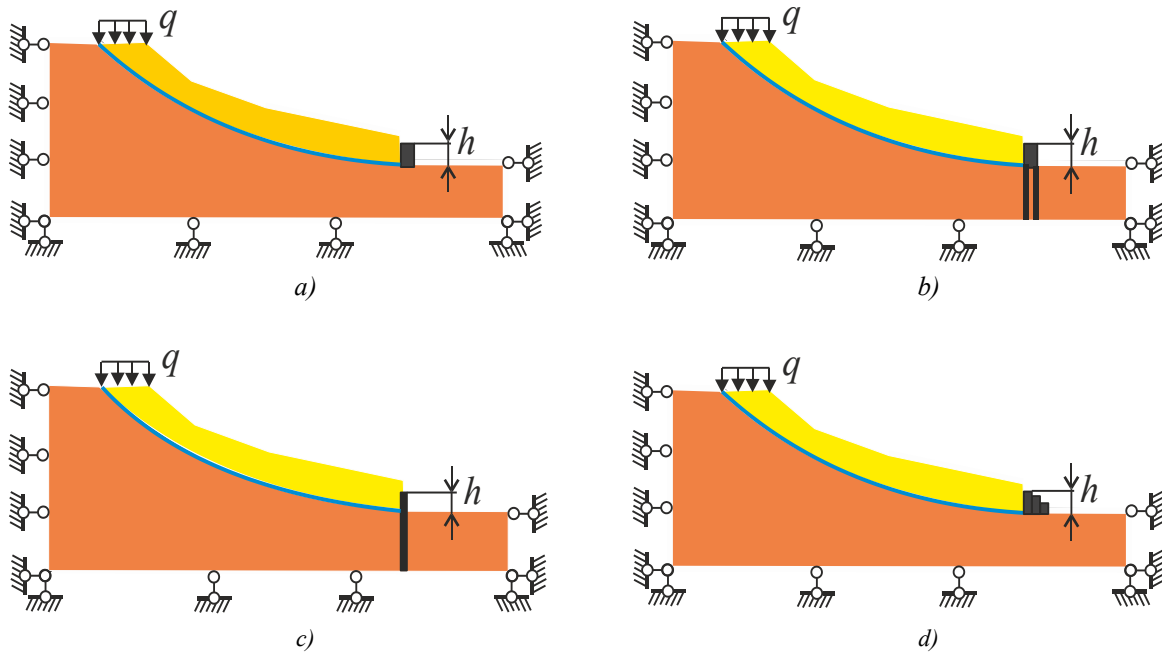


Fig. 12. Schemes of anti-landslide structures:
 a) retaining wall, b) retaining wall on a pile foundation, c) sheet piling, d) gabion

Graphs of changes in horizontal displacements u_x and stresses σ_x along the height h of the considered protective structures are shown in Fig. 14.

Analyzing the results presented, we come to the conclusion that the most pronounced anti-landslide effect from an engineering point of view is scheme *b*, which provides a relatively uniform horizontal displacement of the retaining wall without “collapse”. In this case, maximum horizontal displacement of the wall is 16 mm. To increase the reliability of this design, you can use anchor ties [10].

A certain practical interest in the design of anti-landslide structures is the nature of the distribution of internal forces in the pile foundation. For scheme *b*, the diagrams of the bending moments M occurring in the left and right piles are shown in Fig. 15. The value of the maximum normal compression stress under bending for scheme *b* was $\sigma_{max} = 337 \text{ kN/m}^2$, which is significantly less than the compressive strength of concrete (25.5 MPa).

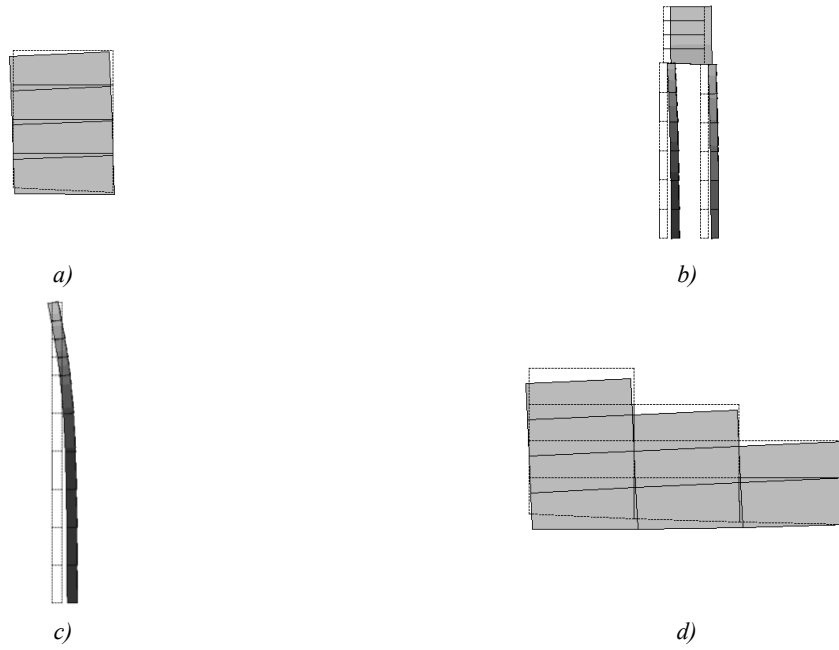


Fig. 13. Visualization of protective structures in the deformed state:
 a) retaining wall, b) retaining wall on a pile foundation, c) sheet piling, d) gabion

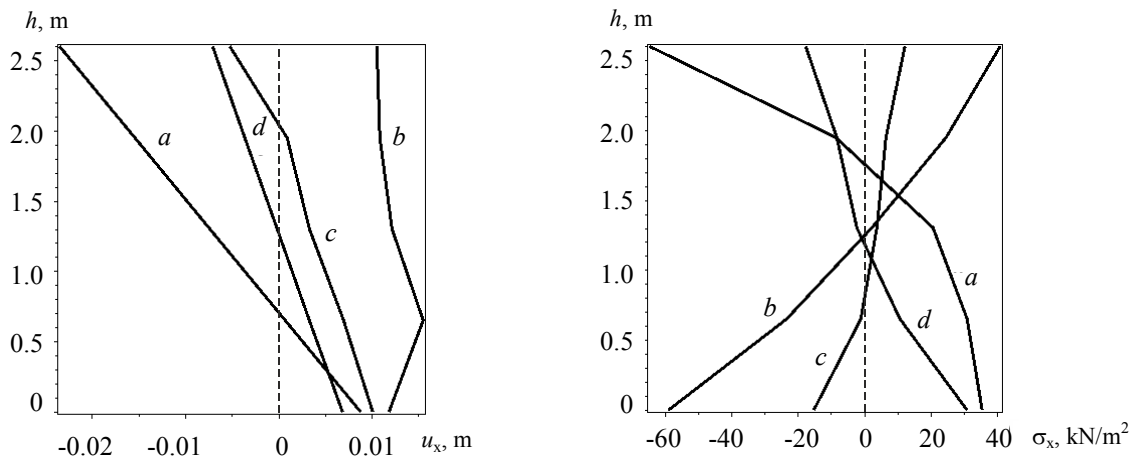


Fig. 14. Graphs $u_x \sim h$ and $\sigma_x \sim h$ for protective structures:
 a) retaining wall, b) retaining wall on a pile foundation, c) sheet piling, d) gabion

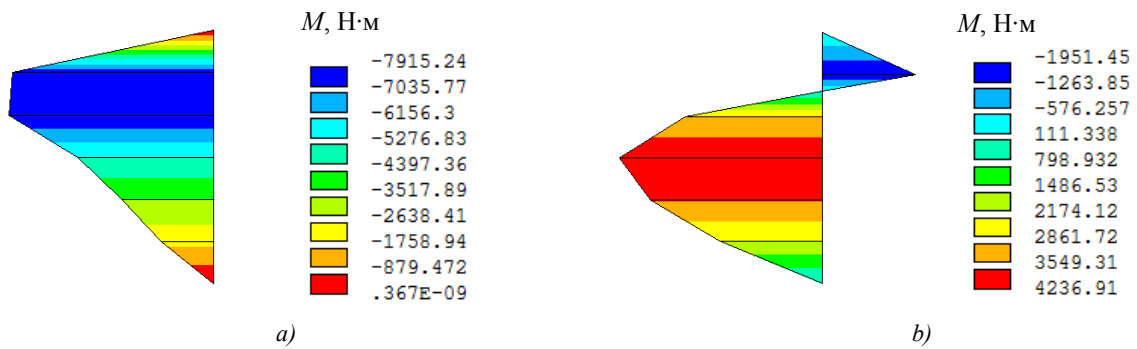


Fig. 15. Diagrams of bending moments in piles of scheme *b* in Fig.12:
 a) left pile; b) right pile

Diagrams of shear forces Q in piles are shown in Fig. 16.

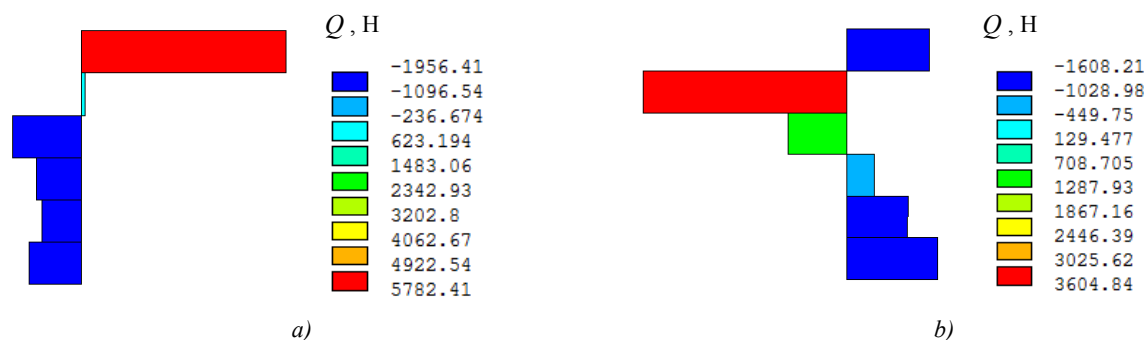


Fig. 16. Diagrams of shear forces in piles of scheme *b* in Fig. 12:
a) left pile; b) right pile

Fig. 16 shows that the cross-section of a possible pile cut is located below the zero mark of the structure.

Discussion and Conclusions. Under the problem of plane deformation, a finite element model is constructed that simulates the landslide process of a natural slope. In contrast to the existing methods of calculating landslide structures, this approach implements the concept of kinematic instability of the landslide layer, the essence of which is to use combined finite elements along the assumed sliding line. A series of numerical experiments was used to test the proposed method for studying the interaction of a sliding landslide and various types of protective structures. It is established that the most effective anti-landslide protection at the given geometric and physical parameters is provided by a combined structure consisting of a retaining wall and a pile foundation.

References

1. Seyed-Kolbadi SM, Sadoghi-Yazdi J, Hariri-Ardebili MA. An improved strength reduction-based slope stability analysis. *Geosciences*. 2019;9(1):55. <https://doi.org/10.3390/geosciences9010055>
2. Griffiths DV, Marquez RM. Three-dimensional slope stability analysis by elasto-plastic finite elements. *Geotechnique*. 2007;57(6):537–546. <https://doi.org/10.1680/geot.2007.57.6.537>
3. Jing Xi Chen, Peng Zhen Ke, Guang Zhang. Slope stability analysis by strength reduction elasto-plastic FEM. *Key Eng. Mater.* 2007;345:625–628. <https://doi.org/10.4028/www.scientific.net/KEM.345-346.625>
4. Mikhailov VO. Trekhmernaya matematicheskaya model' obval'nykh protsessov [3D mathematical model of landfall processes]. *Moscow University Bulletin. Series 5, Geography*. 2011;4:53–58. (In Russ.)
5. Yossef H. Hatzor, Guowei Ma, Gen-hua Shi. *Discontinuous Deformation Analysis in Rock Mechanics Practice*. ISRM, CRC Press, 2018. 410 p.
6. Morozov EM, Muzemnek AY, Shadskii AS. ANSYS v rukakh inzhenera. *Mekhanika razrusheniya [ANSYS is in the hands of an engineer. Destruction mechanics]*. Moscow: LENAND; 2008. 456 p. (In Russ.)
7. Drucker DC, Prager W. Soil Mechanics and plastic analysis or limit design. *Quarterly of Applied Mathematics*. 1952;10(2):157–165.
8. Fadeev AB. *Metod konechnykh ehlementov v geomekhanike [Finite element method in Geomechanics]*. Moscow: Nedra; 1987. 221 p. (In Russ.)
9. Gaigerov PP, Al-Jabobi Sami Fahl, Al-Yaj Mahmoud Abdo Hasa. Konechno-ehlementnoe modelirovanie peredachi usiliya natyazheniya stal'nogo kanata na beton [Finite element modeling of force transmission the tension of the steel tendon on the concrete]. *University News. North-Caucasian region. Technical Sciences Series*. 2017;2:73–78. (In Russ.)
10. Matsii SI, Ryabukhin AK. Svaino-ankernye protivopolznevye konstruksii [Pile-anchor anti-landslide structures]. Krasnodar: KubGAU; 2017. 189 p. (In Russ.)

Received 10.03.2021

Revised 02.04.2021

Accepted 13.04.2021

About the Authors:

Gaidzhurov, Petr P., professor of the Engineering Mechanics Department, Don State Technical University (1, Gagarin sq., Rostov-on-Don, RF, 344003), Dr.Sci. (Eng.), ORCID: <https://orcid.org/0000-0003-3913-9694>, gpp-161@yandex.ru

Saveleva, Nina A., senior lecturer of the Engineering Mechanics Department, Don State Technical University (1, Gagarin sq., Rostov-on-Don, RF, 344003), ORCID: <https://orcid.org/0000-0002-8702-5168>, ninasav86@mail.ru

Dyachenkov, Vladimir A., graduate student of the Engineering Mechanics Department, Don State Technical University (1, Gagarin sq., Rostov-on-Don, RF, 344003), snowflash88@gmail.com

Claimed contributorship

P. P. Gaidzhurov: task formulation; discussion of the results. N. A. Saveleva: conducting a review; selection of a method for solving the construction of a mathematical and computer model; computational analysis; computational analysis; discussion of the results. V. D. Dyachenkov: discussion of the results.

All authors have read and approved the final manuscript.